Brownian motion in dynamically disordered media

James B. Witkoskie, Shilong Yang, and Jianshu Cao*
Department of Chemistry, Massachusetts Institute of Technology, Cambridge, Massachusetts 02139
(Received 22 April 2002; revised manuscript received 12 August 2002; published 26 November 2002)

The motion of Brownian test particles in a model random potential with time dependent correlations is investigated using four methods: renormalized perturbation, perturbation using Martin, Siggia, and Rose functional formalism (MSR), the Edwards variational method on the MSR functional, and renormalization group with the MSR function. The disorder averaged one-particle propagators determined by the renormalized perturbation expansion and MSR perturbation expansion are identical to the second and possibly higher order, and the two-particle propagators determined by these perturbation methods are identical at the first and possibly higher order. The one-particle propagator determined by the Edwards method is identical to the perturbation expansions at the first order, but the second-order analogue of the Edwards method has a more complex expression, which reduces to the second-order perturbation expression with additional higher-order terms. The diffusion constant and two-particle correlations are calculated from these propagators and are used to determine the effects of the random potential on the Brownian particles. Generally, the diffusion rate decreases with the disorder strength and increases with the temporal decay rate. The two competing mechanisms result in an enhancement of the diffusion constant for weak potentials with fast temporal fluctuations. The system exhibits two-particle correlations that are inherently non-Gaussian and indicate clustering behavior. The diffusion constant is also determined from a simple one-loop renormalization group calculation. In the static limit, the diffusion constant calculated by the renormalization group recovers the results of Deem and Chandler [M.W. Deem and D. Chandler, J. Stat. Phys. **76**, 911 (1994)].

DOI: 10.1103/PhysRevE.66.051111 PACS number(s): 05.40.−a, 61.41.+e, 64.70.Pf

I. INTRODUCTION

Many stochastic problems can be modeled by the diffusion of Brownian particles interacting with a random potential [1]. Although there is a macroscopic homogeneous environment, the mesoscopic heterogeneity caused by local environments often plays the central role of determining how the system behaves even on long-time and length scales [2]. Several references have treated random media problems both analytically and numerically to find modifications to the diffusion constant to capture long-time behavior. An interesting issue that is not always examined are the deviations from the Gaussian behavior expected in the intermediate time scales of these random media problems [1–13].

New single molecule experiments examine these mesoscopic time-scale and length scale deviations from Gaussian behavior [14–16]. On these length scales, the random fluctuations of the solvent that influence the motion of the molecule cannot be modeled with the assumption that they are locally correlated in time and space since some large-scale motions of the solvent are on the time scale of the experiment. A result of these nonlocal correlations is deviation from Gaussian behavior on intermediate time scales, which are measured in several experiments [14,15,17,18].

The heterogeneity on mesoscopic length and time scales has physical significance that is observable in experiments and simulations of many systems including systems near phase transitions such as glasses and supercritical fluids.

1. Glasses

Several experiments in glasses demonstrate the effect of the heterogeneous fluctuating environments on molecules, including video microscopy, neutron scattering, NMR, and single-molecule tracking [16,17,19–21]. These experiments are particularly interesting because of the many single-molecule experiments performed on glassy systems. The systems exhibit regions of varying relaxation dynamics as well as collective behaviors, which lead to deviations from Gaussian behavior [17,18,22–26]. Kirkpatrick *et al.* attributes these varying dynamics to the constant formation and destruction of glassy clusters [27]. Experiments on colloidal systems by Weeks *et al.* and members of the Rice group show strong spatio-temporal correlations in the system. Particles in these colloidals system move collectively resulting in long-time correlations [18,22,28,29]. Measurements of the rotational diffusion constants of colloidal spheres in glassy systems show similar strong spatio-temporal correlations [30,31].

2. Supercritical fluids

Diffusion in supercritical fluids is another interesting example of dynamics in heterogeneous environments. The density of supecritical fluids has long length and time-scale correlations, which lead to several anomalous experimental results [32–35]. Although results differ, several experiments report dramatic changes in the diffusion constant of solutes in supercritical fluids [36,37]. These density fluctuations have been observed in MD simulations and persist for long-time scales [34,38,39].

These experiments and simulations show that there are intermediate length and time-scale environmental fluctuations in several interesting systems, which motivates our

*Electronic address: jianshu@mit.edu

study of a stochastic potential with intermediate scale correlations. Because two different stochastic processes, simple diffusion and the random potential, determine the movement of our Brownian particle, we expect significant deviations from the Gaussian form predicted by Einstein's equation. These deviations have been observed and quantified in several simulations and theories [18]. Several references showed that the simple assumption of fluctuating regions of two different diffusion constants, one for a cluster and another for free diffusion, results in significant changes in the diffusion constant and deviations from Gaussian behavior on intermediate time scales [40–42]. Mode coupling theory also predicts significant deviations from the expected Gaussian behavior, especially for glasses [22,29,43–45]. Simulations by Donati *et al.* support these theoretical predictions of non-Gaussian behavior at intermediate times for glasses. Similar to the arguments of Kirkpatrick *et al.* they attribute these deviations to the formation of clusters [25–27]. Motivated by the observations of Donati and others we examine a simple model that exhibits similar clustering behavior.

A. The diffusion model

In order to address this Brownian motion problem analytically, we do not explicitly include the solvent. Instead, we develop a phenomenological model that captures the interactions of the solvent molecules with the Brownian particle without explicitly including them. In this paper, the microscopic time-scale fluctuations are still approximated as simple diffusion, but we extract the larger time-scale motions and write them as a fluctuating potential with a time and spatial dependence. The approach follows the work of Deem and Chandler and has been discussed by Bouchaud and Georges but is generalized to allow a time dependent potential [2,9]. This type of diffusion process is governed by the equation

$$\frac{\partial G(\mathbf{x},t)}{\partial t} = D_0 \nabla^2 G(\mathbf{x},t) + \beta D_0 \boldsymbol{\nabla} \cdot (G(\mathbf{x},t) \boldsymbol{\nabla} V(\mathbf{x},t)), \tag{1.1}$$

with

$$G(\mathbf{x},0) = \delta(\mathbf{x}),$$

where $G(\mathbf{x},t)$ is the Green's function, D_0 is the diffusion constant modeling the short-time-scale interactions, β is the inverse temperature and $V(\mathbf{x},t)$ is the random potential [2,9,10]. The difficulty in dealing with the random media problem is attempting to average $G(\mathbf{x},t)$ over the disorder of $V(\mathbf{x},t)$, even though we assume we know the moments of $V(\mathbf{x},t)$ [9]. In this paper, we will make a Gaussian assumption for the random potential with

$$\langle V(\mathbf{x},t) \rangle = 0$$

and

$$\langle V(\mathbf{x_1},t_1) V(\mathbf{x_2},t_2) \rangle = \chi(|\mathbf{x_1}-\mathbf{x_2}|,|t_1-t_2|) \neq 0. \tag{1.2}$$

All other moments are either zero or can be expressed as a polynomial of χ. This assumption eases computation, but higher order cummulants can be incorporated using the methods below. Most of the equations in this paper are valid for arbitrary χ, but the explicit calculations used to generate the figures will correspond to three dimensions with χ defined by

$$\chi(|\mathbf{x}|,|t|) = \frac{\alpha^{3/2}\chi_0}{(\alpha+\lambda|t|)^{3/2}} \exp\left[- \frac{|\mathbf{x}|^2}{4(\alpha+\lambda|t|)} \right]. \tag{1.3}$$

This potential-potential correlation is chosen because it has some of the features expected for a real potential of a fluid-like system, but it is a model that also allows easier computation. Two of the important aspects of this paper are the various techniques used to derive the Green's functions, the equivalence between them and idea that the potential can mediate the clustering behavior of the system.

The constant $\chi_0 = \chi(|\mathbf{x}|=0,\ t=0)$, corresponds to the strength of the large-scale interactions and is our perturbation expansion parameter. The choice of a Gaussian form allows us to omit a cutoff frequency that separates the small-scale motions that we approximate as simple diffusion from those that we treat as the stochastic potential. $\sqrt{\alpha}$ is the length scale of the heterogeneity of the system, which can be viewed as the size of wells in the potential energy surface. We refer to $\alpha^{d/2}$ as the size of the cluster to make contact with previous experiments and simulations [17,24]. We incorporate decay of spatial correlation into our model by including the $\lambda|t|$ term. The $1/(\lambda|t|)$ dependence is chosen to give an exponential time dependence in Fourier space. This formulation corresponds to smaller-scale fluctuations or clusters decaying faster than larger-scale ones, a property prescribed by Trajus and Kielson [46]. In analogy with several references, we refer to λ as the hopping rate, but we also emphasize the power-law dependence of our potential correlation function does not have a well-defined rate and, even for a strong disorder, the hopping fluctuations in the potential may not be associated with hopping of the Brownian particle since the particle has inertial mass [24,47,48].

B. Summary and outline

In the examination of the random media problem, a self-consistent equation for the one-particle Green's function that is accurate to second order in the disorder strength can be determined by a perturbation expansion of Eq. (1.1) directly [4–7]. But many papers calculated the Green's function and the diffusion constant by using the classical field formalism developed by Martin, Siggia, and Rose (MSR) [1,2,11,12,49]. To show the consistency of our perturbation method with the field theoretic methods of MSR, we solve for the Green's function using both methods and derive equations that are identical up to second order in the disorder strength. This result should not be surprising since both methods attempt to describe the dynamics by a Dyson and Schwinger equation with self-energy. To make contact with previous work, we also solve the equations with an Edwards type of variational method that circumvents the Dyson and

Schwinger equations [2,1]. The variational method yields results that are similar to the our perturbation expansions, as well as previous work but slightly more complex than perturbation. In the static limit the equations are identical to those derived by Deem and Chandler [1,2,10,11,49,50].

The paper also contains a first order equation for the two-particle propagator determined by both the MSR and direct perturbation methods. Hydrodynamic and excluded volume interactions are not considered in this paper since the two-particle propagator is intended to measure variation in different particle trajectories caused by the potential. As seen from Eqs. (2.4) and (5.12) below these results are identical to first-order. As a final result, we use the MSR method to determine a first order renormalization group (RG) calculation of the diffusion constant, which compares well with our perturbation equations and reduces to previous RG calculations in the static limit [2,11].

Our results are organized into six sections. Renormalized perturbation and numerical results are presented in Secs. II–IV followed by the conclusions in Sec. VII. Readers interested in a more detailed discussion of MSR and RG are referred to Secs. V and VI.

II. DETERMINATION OF THE GREEN'S FUNCTION FROM DIRECT PERTURBATION

A. One-particle propagator

To begin our analysis, we perform a direct perturbation and resummation of the Green's function equation to get a second-order self-consistent equation, which we compare with our field theoretic results. The renormalized perturbation expansion is analogous to the direct interaction approximation used to describe turbulent flows [3,8,10,51,52]. Fourier transforming the spatial variables ($\mathbf{x}\rightarrow\mathbf{k}$) gives the equation

$$\frac{\partial}{\partial t}G(\mathbf{k},t)=-D_0|\mathbf{k}|^2G(\mathbf{k},t)-\frac{(\beta D_0)}{(2\pi)^d}\int d\mathbf{h}\{\mathbf{k}\cdot(\mathbf{k}-\mathbf{h})\times(G(\mathbf{h},t)V(\mathbf{k}-\mathbf{h},t))\},\tag{2.1}$$

with

$$G(\mathbf{k},0)=1.$$

The integration over $\mathbf{h}$ runs from $-\infty<|\mathbf{h}|<\infty$. We define $\partial_t+D_0|\mathbf{k}|^2$ as $G_0^{-1}(\mathbf{k},t)$, and $G_0(\mathbf{k},t)$ as our usual fundamental solution for free diffusion,

$$G_0=\exp(-D_0t|\mathbf{k}|^2).$$

With this definition of $G_0(\mathbf{k},t)$ the propagator for a specific realization of disorder is

$$G(\mathbf{k},t)=G_0(\mathbf{k},t)-\frac{(\beta D_0)}{(2\pi)^d}\int d\mathbf{h}d\tau\{\mathbf{k}\cdot(\mathbf{k}-\mathbf{h})V(\mathbf{k}-\mathbf{h},\tau)\times G_0(\mathbf{k},t-\tau)G(\mathbf{h},\tau)\},\tag{2.2}$$

where τ has a range from 0 to t. Repetitively substituting the right-hand side of Eq. (2.2) for $G(\mathbf{k},t)$ in the right hand side of the Eq. (2.2) produces a perturbation expansion for $G(\mathbf{k},t)$ in terms of $V(\mathbf{k},t)$ and $G_0(\mathbf{k},t)$. Since $G_0(\mathbf{k},t)$ has no dependence on the random potential $V(\mathbf{k},t)$, we are able to average over $V(\mathbf{k},t)$ in this expression using Gaussian factorization. We resum terms so that the equation is accurate to various powers of the disorder strength χ_0 and express these terms as self-consistent equations of $G(\mathbf{k},t)$. The resummation procedure corresponds to evaluating the self-energy in the Dyson expansion. The resulting second-order expression is

$$\begin{aligned}\langle G(\mathbf{k},t)\rangle=G_0(\mathbf{k},t)&-\frac{(\beta D_0)^2}{(2\pi)^d}\int d\mathbf{h}d\tau_1d\tau_2\{\mathbf{k}\cdot(\mathbf{k}-\mathbf{h})\mathbf{h}\cdot(\mathbf{k}-\mathbf{h})\chi(|\mathbf{k}-\mathbf{h}|,|\tau_1-\tau_2|)G_0(\mathbf{k},t-\tau_1)\langle G(\mathbf{h},\tau_1-\tau_2)\rangle\langle G(\mathbf{k},\tau_2)\rangle\}\\&+\frac{(\beta D_0)^4}{(2\pi)^{2d}}\int d\mathbf{h_1}d\mathbf{h_2}d\tau_1d\tau_2d\tau_3d\tau_4\{\mathbf{k}\cdot(\mathbf{k}-\mathbf{h_1})\mathbf{h_2}\cdot(\mathbf{k}-\mathbf{h_1})\mathbf{h_1}\cdot(\mathbf{k}-\mathbf{h_1})(\mathbf{k}-\mathbf{h_1})\cdot(\mathbf{k}-\mathbf{h_1}+\mathbf{h_2})\chi(|\mathbf{k}-\mathbf{h_1}|,|\tau_1-\tau_3|)\\&\times\chi(|\mathbf{h_1}-\mathbf{h_2}|,|\tau_2-\tau_4|)G_0(\mathbf{k},t-\tau_1)\langle G(\mathbf{h_1},\tau_1-\tau_2)\rangle\langle G(\mathbf{h_2},\tau_2-\tau_3)\rangle\langle G(\mathbf{k}-\mathbf{h_1}+\mathbf{h_2},\tau_3-\tau_4)\rangle\langle G(\mathbf{k},\tau_4)\rangle\},\end{aligned}\tag{2.3}$$

where the second term is the first-order correction and the third term is the second order correction. The integrations in this expression are for $t>\tau_1>\cdots>\tau_n>0$ and $-\infty<|\mathbf{h_i}|<\infty$ and the $\langle\cdots\rangle$ represents the average over the disorder. The origin of the self-consistent equation can be easily demonstrated with a Feynman diagrammatic expansion and resummation used in QED [53]. In these diagrams, we replace the propagator for photons with the propagator for χ and only use graphs that do not violate causality.

Although the sum of all graphs should converge to the solution, we are not guaranteed that the sum of any subsequence also converges. This lack of convergence may plague the second-order expression, since the graphs captured by this term are predominantly positive. The difficulty may also be purely numerical in nature due to approximations made in evaluating the second-order expression. In either case, a Páde approximation was used in the numerical calculations to aid in convergence of the solution. The specifics of these approximations are discussed in Sec. III A 2.

B. Two-particle propagator

Single-particle motion is not sufficient to resolve the spatio-temporal correlations built into our model. The Eqs. (2.3) show that the Green's function deviates from the Gaussian form predicted by the free propagator, but the amount of the deviation is difficult to determine from examining the Green's function for the motions of a single particle. To overcome this difficulty we determine a perturbation expansion for a two-particle propagator. Section V B 2 shows the same calculation using the MSR perturbation method. This propagator measures the movement of two particles initially separated by a distance r. The correlation of these two particles determines the deviations from the behavior of two independent particles, which allows us to examine the spatial effects of the stochastic potential. As mentioned above, we are not considering any interactions between the particles, like excluded volume and hydrodynamic effects. Although numerical studies demonstrate the importance of both excluded volume and long-range hydrodynamic interactions between particles in many processes, including the glass transition, we are concerned with the roles of the heterogeneity of the solvent on the correlations between particles [54]. We are also not considering the effects of the particles on the solvent. The correlations we examine are strictly mediated through the potential and can be viewed as a demonstration of the deviations of different realizations of the path of the particle due to the potential if the particle was placed at different locations.

The perturbation calculation for the two-particle propagator starts from the expansion of the original Green's function equation. We do not average over the random potential and all terms are present. The propagator is centered at the origin and is denoted by $G^{(1)}(\mathbf{k_1},t_1)=G(\mathbf{k_1},t_1)$, where the superscript (1) denotes the particle label. We introduce a propagator for the second particle that is displaced from the origin by a vector $\mathbf{r}$ and it is denoted $G^{(2)}(\mathbf{k_2},t_2)=\exp[i\mathbf{k_2}\cdot\mathbf{r}]\cdot G(\mathbf{k_2},t_2)$. Like the propagator centered at the origin, we iteratively expand the equation and do not average the single-particle propagator over the random potential. We multiply the two propagators together and then average over the potential using Gaussian factorization. After resummation, the resulting first-order self-consistent equation has a form that is similar to the equation for the single-particle propagator.

$$\begin{aligned}
&G^{(1,2)}(\mathbf{k_1},t_1=t,\mathbf{k_2},t_2=t)\\
&\quad=\langle G^{(1)}(\mathbf{k_1},t)G^{(2)}(\mathbf{k_2},t)\rangle\\
&\quad=\langle G^{(1)}(\mathbf{k_1},t)\rangle\langle G^{(2)}(\mathbf{k_2},t)\rangle\\
&\qquad-\frac{(\beta D_0)^2}{(2\pi)^d}\int d\mathbf{h}\int_0^t d\tau_1\int_0^t d\tau_2\\
&\qquad\times\{\mathbf{k_1}\cdot(\mathbf{k_1}-\mathbf{h})\mathbf{k_2}\cdot(\mathbf{k_1}-\mathbf{h})\chi(|\mathbf{k_1}-\mathbf{h}|,|\tau_1-\tau_2|)\\
&\qquad\times\langle G(\mathbf{k_1},t-\tau_1)\rangle\langle G(\mathbf{k_2},t-\tau_2)\rangle\\
&\qquad\times G^{(1,2)}(\mathbf{h},\tau_1,\mathbf{k_1}+\mathbf{k_2}-\mathbf{h},\tau_2)\}. \qquad (2.4)
\end{aligned}$$

Two of the propagators are not labeled because they are single-particle propagators with no mulitplication by $\exp[i\mathbf{k}\cdot\mathbf{r}]$ and $\langle G(\mathbf{k},t)\rangle$ corresponds to the single-particle Green's function in Eq. (2.3). This equation can also be represented by a Feynman diagrammatic expansion and resummation [53].

III. DERIVATION OF IMPORTANT STATISTICAL QUANTITIES FROM THE GREEN'S FUNCTIONS

The preceding section outlines the derivation of the self-consistent equations for various Green's functions, which correspond to different possible single-molecule experiments. These experiments measure certain numerical quantities associated with motions of the Brownian particles but they do not measure the Green's functions directly. In this section we outline methods of extracting some measurable quantities from the self-consistent equations derived above, including the diffusion constant and indicators of the deviation of the two-particle Green's function from the uncorrelated motion of two independent particles. We will refer to these quantities as non-Gaussian indicators, but the system is not necessarily Gaussian if these quantities are zero. Several non-Gaussian indicators are possible and we discuss a few that are easily determined from experiments [18,23,25,26].

A. Diffusion constant

1. A simple Ansatz

As discussed in the introduction, macroscopic effects of mesoscopic disorder led to many studies that determine the diffusion constant from self-consistent equations similar those derived above [2,10,11,49,50]. Most of these references address static disorder, but these methods can be generalized for the dynamic case. Our analysis parallels several of these approaches. The methods require numerical computation of the solution from a suitable basis set [2]. Before introducing these rigorous methods, we perform a simple analytic calculation based on a simple Ansatz that the single-particle Green's function maintains a Gaussian form, but the diffusion constant is modified.

$$\langle G(\mathbf{k},t)\rangle\approx\exp[-Dt|\mathbf{k}|^2]. \qquad (3.1)$$

For weak disorder, the Gaussian form is exact and the approximation should determine the correct initial slope of the diffusion constant. The diffusion constant can be expressed in terms of the Laplacian of the Green's function.

$$\lim_{t\to\infty}\left.\frac{-\nabla_{\mathbf{k}}^2 G(\mathbf{k},t)}{2dt}\right|_{\mathbf{k}=0}=D. \qquad (3.2)$$

The Gaussian form allows analytic evaluation of the first-order expression with the Gaussian form of the potential correlation functions, χ in Eq. (1.3), which results in an algebraic expression for the diffusion constant

$$D=D_0-\frac{D_0^2(D-\lambda)}{(D+\lambda)^2}\frac{\beta^2\chi_0}{3}. \qquad (3.3)$$

The equation has no explicit dependence on the cluster size because it is the intrinsic scale of the problem, which determines the magnitude of the other quantities. The equation exhibits the expected behavior from intuition. As the disorder strength χ_0 increases, the diffusion constant will decrease, and as the hopping rate λ increases, the diffusion constant will increase, but this increase is dependent on the disorder strength. If $\lambda > D_0$ the equation suggests an increase in the diffusion constant. This result is not surprising in the weak disorder limit since the forces on the particle increase displacements, but there is no trapping because the potential rearranges quickly and is weak. The solution of this equation as a function of $\beta^2\chi_0/3$ and λ is plotted in Figure 1(a). The RG result is also plotted as a function of $\beta^2\chi_0/3$ and λ in Fig. 1(b). A derivation of the RG result and a more detailed comparison of these results are discussed in Secs. VI and IV respectivley.

2. Numerical determination of the diffusion constant

In order to go beyond the simple assumption of a Gaussian form, we need to implement a numerical approximation method for determining the Green's function and subsequently the diffusion constant. The numerical solutions are calculated in Laplace space using a basis set approach, which is similar to the approach of Deem and Chandler [2]. Approximate first- and second-order solutions using a 16 function basis set were determined as functions of $\beta^2\chi_0/3$ for $\lambda/D_0 = 0.0, 0.4, 1.2$. These results are presented in Figs. 3(a), 3(b), and 3(c) for $\lambda/D_0 = 0.0, 0.4, 1.2$, respectively. These figures also compare the RG calculation and the simple self-consistent result, Eq. (3.3).

The basis set equations are complicated non-linear integral equations that are difficult to solve analytically or numerically. Several numerical approximations used in evaluating these expressions introduce errors other than the choice of the basis set. To aid in convergence with these numerical approximations, a Páde approximation is introduced. This approximation has the correct 1st and 2nd order terms, but also includes additional higher order terms that may aid in convergence. This approximation combines our first- and second-order correction terms in Eq. (2.3).

$$\frac{(\text{first-order expression})}{1-\dfrac{(\text{second-order expression})}{(\text{first-order expression})}}. \tag{3.4}$$

The errors introduced in determining the numerical results are higher than second order in terms of disorder strength so the equation is still accurate at second order. These approximations are not necessary for the $\lambda \to 0$ limit, and a comparison of the numerical solutions with and without the Páde approximation in this limit shows good agreement at moderate disorder strengths. The Páde approximation prevents higher-order terms contained in the first and second renormalized expressions from strongly influencing the fit, which makes our calculation less sensitive to other approximations necessary to numerically calculate the diffusion constant. This is especially important since the terms captured by the second-order expression are predominately positive, which may prevent convergence since we are only summing some graphs. The extra higher-order terms in the Gaussian reference calculation in Eq. (5.14) may also alleviate this sensitivity, as would including higher-order terms in the perturbation expansion. Numerically, both the second-order Gaussian reference calculation and including higher-order perturbation expansion terms would be difficult and is not performed here. A detailed discussion of the results for the calculations performed in this paper is presented in Sec. IV.

B. Non-Gaussian indicators

In order to analyze the non-Gaussian nature of the model, we need to define quantities that measure the deviations from uncorrelated behavior. Experimentally determining deviations from Gaussian behavior is difficult with a single particle, so we analyze the model for two particles that is developed in Sec. II B. The indicators should demonstrate collective motions like clustering because of structures in the system that prevents two particles from moving independently. Both of these effects are observed in experiments and simulations of real systems like glasses [14,18,22,24,25,48].

Two correlations that are measured in several single-molecule experiments are the dot product of the displacement vectors of two-particles initially separated by a distance r, $\delta\mathbf{R}_1 \cdot \delta\mathbf{R}_2$, and the square of the displacements, $\delta\mathbf{R}_1^2 \cdot \delta\mathbf{R}_2^2$ [55,56]. The subscripts label the particle and the δ denotes the displacement from the initial position. The equation for the two-particle propagator is difficult to manipulate because it requires the solution for the one-particle Green's function. To simplify the analysis, we perform an asymptotic expansion of the equations and only evaluate the nonrenormalized terms. To normalize the function, we divide this quantity by $\beta^2\chi_0$. The two corrrelation functions are

$$C_1(r,t) = \frac{\langle \delta\mathbf{R_1}(t) \cdot \delta\mathbf{R_2}(t) \rangle}{(\beta^2\chi_0)\langle |\delta\mathbf{R}|^2 \rangle} \approx \frac{\langle \delta\mathbf{R_1}(t) \cdot \delta\mathbf{R_2}(t) \rangle}{(\beta^2\chi_0)(2dD_0t)}, \tag{3.5}$$

$$C_2(r,t) = \frac{\langle |\delta\mathbf{R_1}(t)|^2 |\delta\mathbf{R_2}(t)|^2 \rangle - \langle |\delta\mathbf{R}|^2 \rangle^2}{(\beta^2\chi_0)\langle |\delta\mathbf{R}|^2 \rangle^2}$$

$$\approx \frac{\langle |\delta\mathbf{R_1}(t)|^2 |\delta\mathbf{R_2}(t)|^2 \rangle - \langle |\delta\mathbf{R}|^2 \rangle^2}{(\beta^2\chi_0)(2dD_0t)^2}. \tag{3.6}$$

To first order these can be written in Fourier space as

$$\frac{(\beta D_0)^2}{(\beta^2\chi_0)(2dD_0t)(2\pi)^d} \nabla_{\mathbf{k_1}} \cdot \nabla_{\mathbf{k_2}} \Bigg(\exp[-i\mathbf{k_2}\cdot\mathbf{r}] \int d\mathbf{h} \int_0^t d\tau_1 \times \int_0^t d\tau_2 \{\mathbf{k_1}\cdot(\mathbf{k_1}-\mathbf{h})\mathbf{k_2}\cdot(\mathbf{k_1}-\mathbf{h})\chi(|k_1-h|,|\tau_1-\tau_2|) \times G_0(\mathbf{k_1}, t-\tau_1) G_0(\mathbf{k_2}, t-\tau_2) G_0(\mathbf{h}, \tau_1) \times \exp[i(\mathbf{k_1}+\mathbf{k_2}-\mathbf{h})\cdot\mathbf{r}] G_0(\mathbf{k_1}+\mathbf{k_2}-\mathbf{h}, \tau_2)\} \Bigg), \tag{3.7}$$

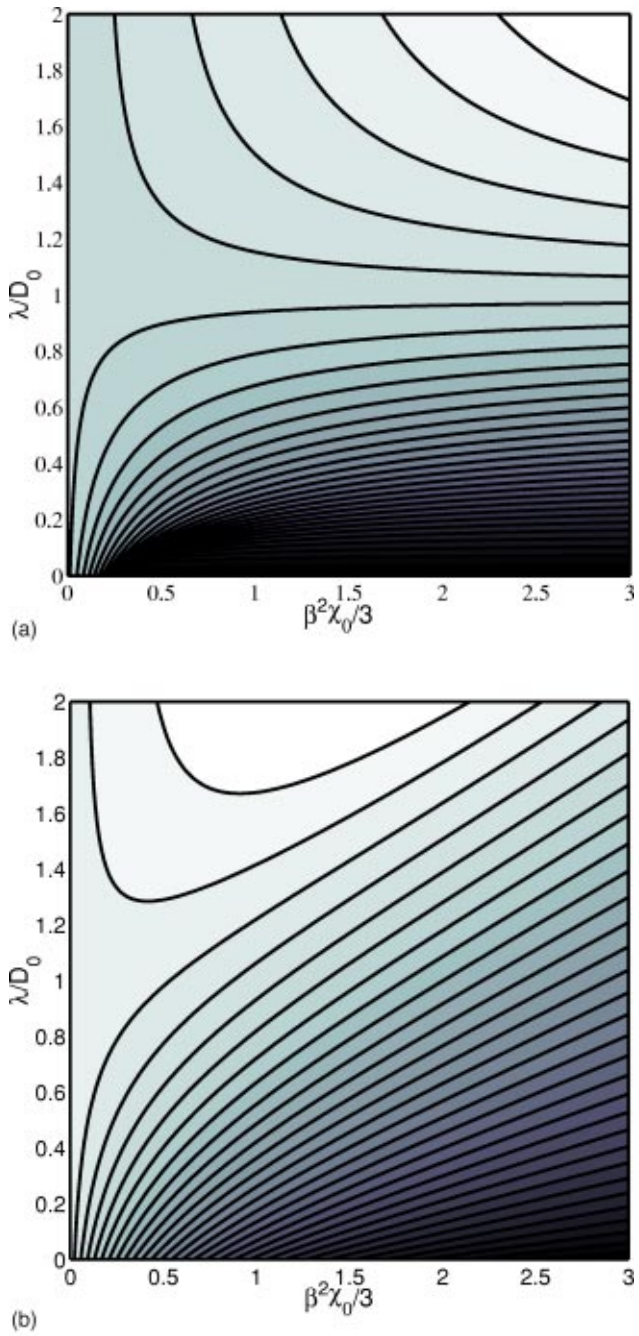

FIG. 1. Contour plot of the diffusion constant as a function of λ and $\beta^2\chi_0/3$ as determined by Eq. (3.3) in (a) and the renormalization group result of Sec. VI in (b).

$$\frac{(\beta D_0)^2}{(\beta^2\chi_0)(2dD_0t)(2\pi)^d}\nabla^2_{\mathbf{k_1}}\nabla^2_{\mathbf{k_2}}\Big\{\exp[-i\mathbf{k}'\cdot\mathbf{r}]\int d\mathbf{h}\int_0^t d\tau_1$$
$$\times\int_0^t d\tau_2\{\mathbf{k_1}\cdot(\mathbf{k_1}-\mathbf{h})\mathbf{k_2}\cdot(\mathbf{k_1}-\mathbf{h})\chi(|\mathbf{k_1}-\mathbf{h}|,|\tau_1-\tau_2|)$$
$$\times G_0(\mathbf{k_1},t-\tau_1)G_0(\mathbf{k_2},t-\tau-2)G_0(\mathbf{h},\tau_1)$$
$$\times\exp[i(\mathbf{k_1}+\mathbf{k_2}-\mathbf{h})\cdot\mathbf{r}]G_0(\mathbf{k_1}+\mathbf{k_2}-\mathbf{h},\tau_2)\}\Big|. \qquad (3.8)$$

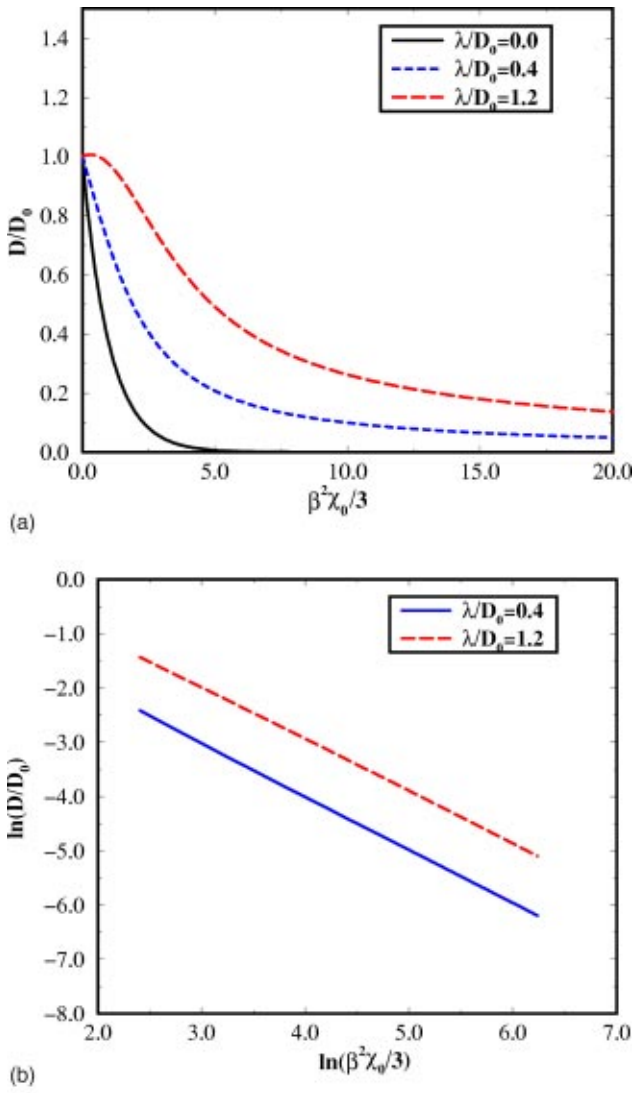

FIG. 2. (a) shows the behavior of the diffusion constant predicted by the renormalization group calculation over large range of disorder strengths for $\lambda/D_0=0.0$,0.4, and 1.2. (b) is a log-log plot of the diffusion constant versus the disorder strength for large disorder for $\lambda/D_0=0.4$ and 1.2. The static limit is not plotted because it is an exponential. The straight line with nearly unity slope shows the power-law dependence of disorder for moderate values of λ

The first correlation C_1 contains both angular and radial information, while C_2 contains only radial information. These quantities are useful in microrheological experiments [55,56]. Because the integral is Gaussian for our model potential, these expressions can be integrated analytically resulting in complex expressions that are omitted. The two correlation functions behave similarly so we only present the features of C_2 in Figs. 4 and 5. These figures are analyzed in Sec. IV.

IV. ANALYSIS OF RESULTS

In the previous section, Sec. III, the diffusion constant and non-Gaussian indicators are defined and determined by renormalized perturbation for the random potential presented

in Eq. (1.3). In this section we present a detailed discussion of the properties of the solutions to compare these results to previous models and demonstrate some of the unusual properties of this model.

A. Diffusion constant

Section III presents several approximations for determining the diffusion constant, and Sec. VI presents a RG approximation of the diffusion constant. Due to the technical nature of the RG calculation, we compare the results of the perturbation and RG calculation in this section before discussing the details of the RG calculation in Sec. VI. The analysis begins by defining $\sqrt{\alpha}$ as our length scale and α/D_0 as our time scale. With the redefinition of our length scales, χ in Eq. (1.3) is uniquely determined by two dimensionless quantities $\beta^2\chi_0/3$ and λ/D_0. All figures and discussions of the effects of the hopping rate λ and the disorder strength χ_0 are in terms of these dimensionless quantities and the diffusion constant is also made dimensionless by dividing by D_0.

Figure 1 presents a contour plot of the solution that is generated from Eq. (3.3) and the RG calculation in Sec. VI. Both plots appear similar for weak disorder strength because they capture the correct first-order response of the diffusion constant. In the weak disorder regime, the diffusion constant is dominated by the disorder strength because the hopping rate's effect on the diffusion constant is proportional to the disorder strength. For moderate hopping rates λ the two figures agree up to stronger disorder strengths because the two equations yield similar results, as long as D stays close to D_0.

For strong disorder strengths, the two equations show markedly different characteristics. For a small hopping rate, the perturbation solution, Eq. (3.3), predicts that the particle becomes trapped for moderate disorder. Because $\chi(0,0)$ is Gaussian, it can never be large and trapping should not occur [57]. The trapping predicted by perturbation expansions is common in disordered media problems because the effect of the disorder is over emphasized [10]. For larger hopping rates, the perturbation result predicts that the diffusion constant approaches the hopping rate, which suggests that the particle is trapped in a well that is moving at the hopping rate. As mentioned previously, a well-defined time constant for the hopping is not defined so this result is as unphysical as the trapping predicted for a small hopping rate.

Unlike the perturbation result, the RG calculation, never predicts trapping. The solution remains above the solution determined by Dean and by Deem, which is above the lower bound determined by Masi *et al.* [2,11,57]. In fact, in the $\lambda \to 0$ limit, the results of Dean and of Deem are recovered [2,11]. For any value of the hopping rate, the diffusion constant approaches zero in the strong disorder limit so the contour lines of Fig. 1(b) never become parallel with the $\beta^2\chi_0/3$ axis. For $\lambda \gg 0$, the diffusion constant approaches zero as a power law, see Fig. 2. Except for small λ, the exponent is weakly dependent on λ and close to unity.

The numerical solutions are more computationally intensive than the simple self-consistent equation, Eq. (3.3), and the RG result so these equations are used to determine the

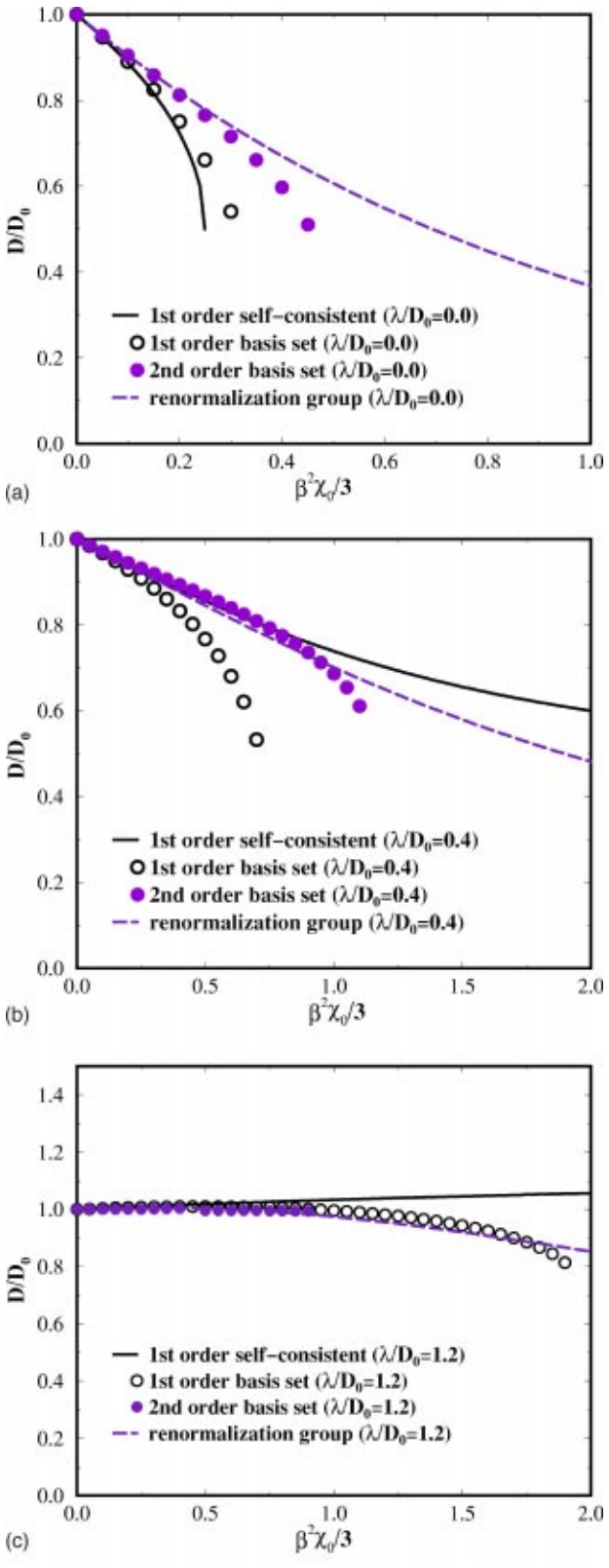

FIG. 3. Comparison of the first-order (empty circles) and second-order (filled circles) numerical solutions derived from the basis set approach outlined in Sec. III A 2 and the results of Eq. (3.3) (solid line), and the renormalization group (RG) (dashed line) for $\lambda/D_0 = 0.0$ in FIG. (a), $\lambda/D_0 = 0.4$ in (b), and $\lambda/D_0 = 1.2$ in FIG. (c).

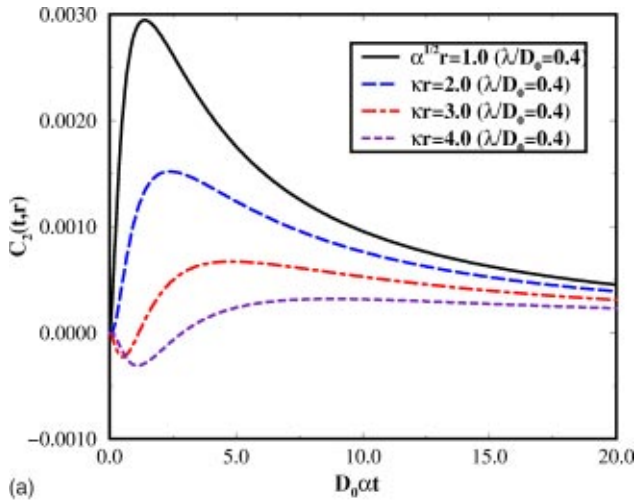

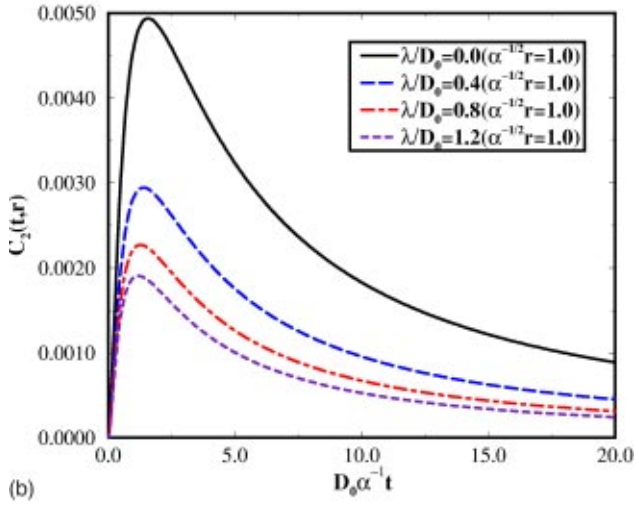

FIG. 4. Time dependence of the non-Gaussian indicator C_2. (a) shows the behavior of C_2 as a function of time for several values of initial separation with $\lambda/D_0=0.4$. (b) shows the behavior of C_2 as a function of time for several values of λ with $r=\sqrt{\alpha}$.

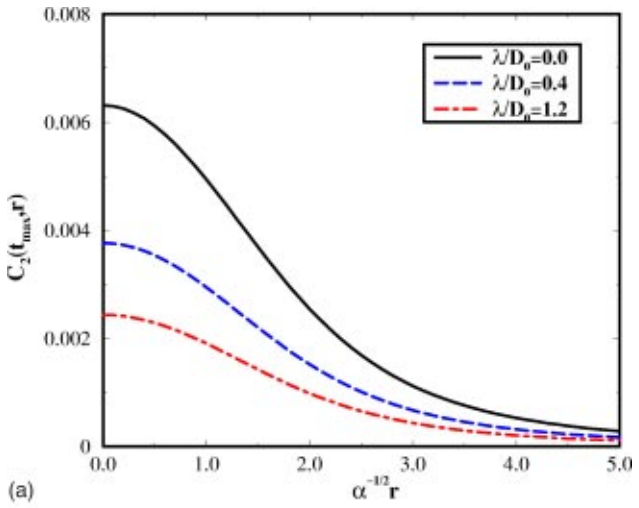

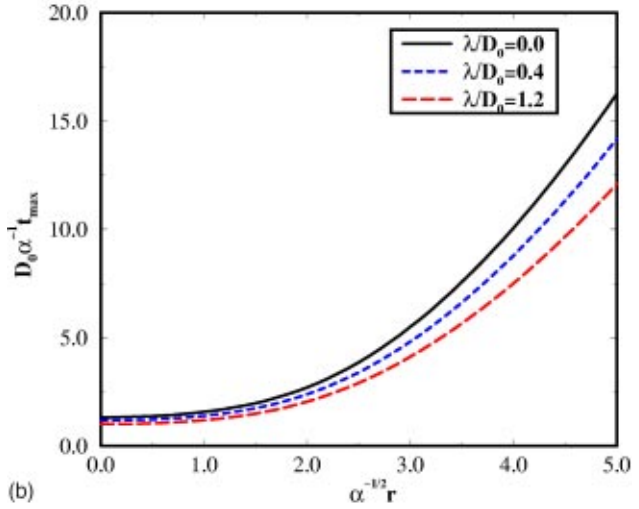

FIG. 5. (a) shows the maximum value of C_2 as a function of initial separation r for several values of λ. (b) shows the time of the maximum. From the figures it is apparent that λ does not qualitatively affect the shape of these graphs.

diffusion constant for specific values of the hopping rate, $\lambda/D_0=0.0,0.4,1.2$. These results are compared against the results of Eq. (3.3) and the RG calculation in Fig. 3. All of the different techniques agree in the small disorder limit, but the numerical calculations predict trapping of the paticle for finite disorder strength for all values of λ. The second-order numerical solution agrees with the RG solution for larger disorder strengths than the first-order numerical solution. The better agreement between the RG and second order solutions for diffusion problems in the static limit has been demonstrated in several papers, and numerical simulations in the static limit suggest that the RG calculation may be correct up to larger disorder strengths than would be expected from a first-order RG result [50,58]. Because of these previous studies, the static disorder results are not surprising, and our RG calculation is a reasonable extension of these previous calculations.

The $\lambda/D_0=1.2$ case demonstrates interesting behavior because nonrenormalized perturbation expansion predicts that the diffusion constant initially increases as discussed above. Because of the power-law time dependence of the potential correlations, one expects stronger disorder strength to eventually restrict the motion of the particle causing a decrease in the rate of diffusion. These intuitive arguments agree with the numerical calculations and the RG result and show that these results capture the physical aspects of the problem. Diffusion initially increases with increasing disorder strength but it eventually decreases in the strong disorder limit.

B. Non-Gaussian indicators

Determining the diffusion constant for disordered media is important in many industrial processes like chromatography, but single-molecule experiments do not study macroscopic diffusion. The experiments study deviations from simple diffusion on intermediate time scales. Although more detailed calculations can be performed, the simple first-order nonrenormalized calculation demonstrates several of the in-

teresting features of this model, including an apparent cluster size and the effect of the dynamics of the random potential, λ [which can be shown from the C_1 calculation in Eq. (4.1) below]. We defined two non-Gaussian indicators in Sec. III B in order to capture the angular and radial dependence of correlations involving two Brownian particles separated by an initial distance r.

The C_1 correlation function contains information that can be interpreted as clustering. Clustering of the two particles would correspond to the particles having a tendency to move together resulting in a decrease in the distance between them as compared to the motions of independent particles. As a result, $\langle|\mathbf{R_1}-\mathbf{R_2)}|^2\rangle$ would be less than the value predicted for independent particles. Because $\langle \mathbf{r}\cdot\delta\mathbf{R_1}\rangle=\langle \mathbf{r}\cdot\delta\mathbf{R_2}\rangle=0$,

$$\begin{aligned}\langle|\mathbf{R_1}-\mathbf{R_2}|^2\rangle &= \langle|\delta\mathbf{R_1}-\mathbf{r}-\delta\mathbf{R_2}|^2\rangle \\ &= \langle|\delta\mathbf{R_1}|^2\rangle+\langle|\delta\mathbf{R_2}|^2\rangle \\ &\quad +|\mathbf{r}|^2-2\langle\delta\mathbf{R_1}\cdot\delta\mathbf{R_2}\rangle. \end{aligned} \tag{4.1}$$

From this expression we see that a positive C_1 means that particles have a tendency to move closer together than predicted by independent motion and a negative C_1 corresponds to the opposite behavior.

The C_2 correlation function is a measure of correlations of the rates of diffusion for the two particles as compared to independent particles. We concentrate our analysis on C_2 because the two functions share similar characteristics with only minor quantitative differences which will be discussed below. Since there are only small differences, the graphs in Figs. 4 and 5 only correspond to the C_2 correlation function. We are examining the nonrenormalized perturbation calculation and all quantities are proportional to the disorder strength. Similar to the diffusion constant, the natural length scale is $\sqrt{\alpha}$ and the natural time scale is α/D_0. Because of these relationships, α, D_0, and $\beta^2\chi_0/3$ are set to unity. The important parameters that have a qualitative effect on the non-Gaussian indicators is the initial separation of the two particles, r, and the dynamics of the potential, λ.

The effect of the initial separation is stronger than the dynamics of the potential since the time dependent factor is also dependent on the spatial factor, $\exp[-|\mathbf{r}|^2/(\alpha+\lambda|t|)]$. For short times, the temporal decay of the spatial correlations is not large and the correlations are completely dominated by the spatial separation. The strong dependence on r is apparent by examining Figs. 4 and 5. For small initial separations, the system shows strong positive correlations for both C_1 and C_2, resulting in a high positive peak. For larger values of r the strength of the correlations decrease and both C_1 and C_2 show anticorrelations in the short time behavior for some values of r. The C_1 correlation shows only a simple inversion for $r>\sqrt{6\alpha}$. As discussed above, negative correlations in C_1 correspond to a larger increase in the distance between the two particles than would be expected for independent particles. The C_2 correlation shows a more complex inverse response. For $1.9\sqrt{\alpha}>r>4\sqrt{\alpha}$ the correlation function shows an intial inverse behavior, but for some values of $r>4\sqrt{\alpha}$ the correlation is intially positive for a short period of time before becoming negative. In the long-time limit, all correlations become positive and decay as power laws, $C_1\propto t^{-1}$ and $C_2\propto t^{-3/2}$. The power-law behavior comes from the normalization of the correlation functions, but it demonstrates that the correlations between the two particles remains significant even at large times.

Unlike the strong qualitative effect of the initial separation, the time dependence of χ only affects the quantitative features of the correlation functions. The qualitative shapes of the correlations do not change, but the height and positions of the maxima changes as λ changes. The time and height of the maxima of C_2 as a function of r for several values of λ are presented in Fig. 5, which demonstates the qualitative effects of r and the quantitative effects of λ.

The strong positive correlations between particles separated by small distances suggest that the model does exhibit clustering behavior. The particles that are within $\sqrt{6\alpha}$ diffuse with similar speeds and have a tendency to move closer together than expected if they are uncorrelated. This behavior is similar to what is expected for particles in the ''same cluster.'' If the particles are farther apart than the length of a cluster, they are in two ''different clusters,'' which have a tendency to diffuse away from each other, leading to negative correlation in C_1.

V. MSR FIELD THEORY

The perturbation expansion equations can be derived using the MSR formalism [59–61]. But most applications of MSR to diffusion problems have been centered around RG calculations and reference systems [2,9,11]. These efforts are stimulated by the quenched disorder problems where the Green's function instead of the generating function should be averaged over quenched disorder [9]. As stated in the Introduction, Sec. I, the nontrivial terms for this particular problem are the same regardless of averaging over the generating function or the Green's function so we examine the perturbation expansion of this problem, as well as a reference and RG calculation. This equivalence between the different averaging techniques for certain dynamic problems has been discussed elsewhere, and should not be surprising since the system will always be diffusive [1,2,57,62–64]. For a more detailed discussion of MSR we refer readers to several references [1,2,59–63,65–71].

A. The generating function

To write the random media problem into the field theoretic formalism we note that the diffusion equation is also the equation for the change in the probability density at a point in space. With this idea we can write a replica generating function in a form that is similar to a Feynman path intgral. Defining

$$\begin{aligned} G_0^{-1}(\hat{\mathbf{1}},\mathbf{2}) &= \delta(\mathbf{1}-\mathbf{2})(\partial_{t_2}+D_0|\mathbf{k_2}|^2) \\ &= \delta(\mathbf{1}-\mathbf{2})(-\partial_{t_1}+D_0|\mathbf{k_1}|^2) \end{aligned} \tag{5.1}$$

and

$$\gamma(\hat{\mathbf{1}},\mathbf{2},\hat{\mathbf{3}},\mathbf{4}) = \frac{(\beta D_0)^2}{(2\pi)^d}\delta(t_1-t_2)\,\delta(t_3-t_4)\,\delta(\mathbf{k_1}-\mathbf{k_2}+\mathbf{k_3}-\mathbf{k_4}) \times \mathbf{k_1}\cdot(\mathbf{k_1}-\mathbf{k_2})\mathbf{k_3}\cdot(\mathbf{k_3}-\mathbf{k_4})\chi(|\mathbf{k_1}-\mathbf{k_2}|,|t_1-t_3|)$$

the generating function is

$$Z^N[\xi_i,\hat{\xi}_i] = \int \mathcal{D}[\rho_i]\mathcal{D}[\hat{\rho}_i]\exp\Big[-G_0^{-1}(\hat{\mathbf{1}},\mathbf{2})\hat{\rho}_i(\mathbf{1})\rho_i(\mathbf{2}) + \frac{1}{2}\gamma(\hat{\mathbf{1}},\mathbf{2},\hat{\mathbf{3}},\mathbf{4})\hat{\rho}_i(\mathbf{1})\rho_i(\mathbf{2})\hat{\rho}_j(\mathbf{3})\rho_j(\mathbf{4}) + \xi_i(\mathbf{1})\rho_i(\mathbf{1}) + \hat{\xi}_i(\mathbf{1})\hat{\rho}_i(\mathbf{1})\Big], \tag{5.2}$$

where we integrate over repeated arguments and sum over indices i and j [2,61]. The notation we use in Eq. (5.2) is consistent with Jensen's work. The variables $\mathbf{1}=[\mathbf{k_1},t_1]$ and $\mathbf{2}=[\mathbf{k_2},t_2]$ stand for all variable parameters, like space and time and the components of these variables are denoted with a subscript, 1 or 2. This generating function introduces a conjugate variable $\hat{\rho}(\mathbf{1})$, which acts as an infinitesimal density creation operator. Differentiation of $\ln Z$ with respect to $\xi_i(\mathbf{1})$ and $\hat{\xi}_i(\mathbf{1})$ determines the desired statistical quantities. For the perturbation expansion we take $N=1$ since we are averaging over the generating function. In the reference calculation, where the Green's function is averaged, the $N\to 0$ limit is taken in the replica action, which eliminates several terms that are present in the $N=1$ limit. It may appear that the two different limits cannot both be correct, but the additional terms in the perturbation expansion that are eliminated in the $N\to 0$ limit are noncausal and evaluate to zero as discussed above [62,63]. This result gives us confidence that our MSR perturbation, where we do not take the $N\to 0$ limit, does not fail to properly average over the disorder [9]. The η is the Jacobian which depends on discretization and can be assumed to be constant.

The action in Eqs. (5.2) is very similar to the actions in other references on diffusion in random media [2,9,10,50,58]. Our derivation is for the general case of dynamic disorder and our equations simplify to these previous results in the static limit. Because we consider dynamics, we must integrate over time or frequency, which can often be omitted in the static case [2]. Some slight differences also come from our definition of $\hat{\rho}$, which is equal to $-i\hat{\rho}$ in several references [2,12,13,72]. The largest contrast comes from our action being defined in Fourier space so the signs of some of the arguments, like **2** are reversed. Because of the domain of definition, the Fourier transform of $\hat{\rho}$ corresponds to density created at a specific wave vector instead of a specific point in space.

The generating function gives us all of the desired statistical quantities by differentiating $\ln Z[\xi_i,\hat{\xi}_i]$ with respect to the generating variables ξ_i and $\hat{\xi}_i$. The replica trick that we use in our Gaussian reference calculation replaces the $\ln Z[\xi,\hat{\xi}]$ with $\lim_{N\to 0}(Z^N-1)/N$, but we are still evaluating the same quantities. The Green's function is defined by

$$\langle\langle \rho(\mathbf{1})\hat{\rho}(\mathbf{2})\rangle\rangle = G_2(\mathbf{1},\hat{\mathbf{2}}) = \left.\frac{\delta^2 \ln Z[\xi_i,\hat{\xi}_j]}{\delta\xi_i(\mathbf{1})\,\delta\hat{\xi}_j(\mathbf{2})}\right|_{\xi_i=\hat{\xi}_j=0}. \tag{5.3}$$

This quantity is the response function and it represents the creation of density at the wave vector $\mathbf{k_2}$ at time t_2 and subsequently measuring the density at the wave vector $\mathbf{k_1}$ at time t_1, which is similar to the definition of the Green's function defined in Eq. (1.1), except that the density creation is defined in Fourier space.

B. MSR perturbation theory

1. One-particle propagator

The perturbation method follows the derivation of Jensen [61]. We explicitly construct Schwinger and Dyson equations from $Z[\xi,\hat{\xi}]$ instead of evaluating $\ln Z[\xi,\hat{\xi}]$. $N=1$ and we are not introducing the unphysical replica trick. We also introduce the Legendre transform variable Γ,

$$\Gamma[G_1,\hat{G}_1] = \ln Z[\xi,\hat{\xi}] - \xi(\mathbf{1})G_1(\mathbf{1}) - \hat{\xi}(\mathbf{1})G_1(\hat{\mathbf{1}}), \tag{5.4}$$

where $\mathbf{i}$ and $\hat{\mathbf{i}}$ refer to $\rho(\mathbf{i})$ and $\hat{\rho}(\mathbf{i})$, respectively. When the variable is either $\rho(\mathbf{i})$ or $\hat{\rho}(\mathbf{i})$ it appears as $\tilde{\mathbf{i}}$. The Legendre transform formally closes the Dyson's equation. Note that the Green's functions generated by $Z[\xi,\hat{\xi}]$ are already averaged over the random potential and the $\langle\cdots\rangle$ is omitted . We assume that $\Gamma_2(\tilde{\mathbf{1}},\tilde{\mathbf{2}}) = -G_2^{-1}(\tilde{\mathbf{1}},\tilde{\mathbf{2}})$. This equality is not necessarily strict but it allows simple manipulation of the equations. The equations derived by MSR allow us to use perturbation theory to systematically expand and evaluate the self-energy, as demonstrated by Deker [65–67]. The resulting set of equation are

$$G_2(\mathbf{1}',\hat{\mathbf{1}}'') = G_0(\mathbf{1}',\hat{\mathbf{1}}'') + G_0(\mathbf{1}',\hat{\mathbf{1}})\,\gamma(\hat{\mathbf{1}},\mathbf{2},\hat{\mathbf{3}},\mathbf{4}) \times[G_2(\mathbf{2},\hat{\mathbf{5}})G_2(\hat{\mathbf{3}},\mathbf{6})G_2(\mathbf{4},\hat{\mathbf{7}})G_2(\hat{\mathbf{1}}'',\mathbf{8}) \times\Gamma_4(\hat{\mathbf{5}},\mathbf{6},\hat{\mathbf{7}},\mathbf{8}) + G_2(\mathbf{2},\hat{\mathbf{3}})G_2(\mathbf{4},\hat{\mathbf{1}}'')], \tag{5.5}$$

$$\Gamma_2(\mathbf{1}',\hat{\mathbf{1}}'') = -G_2^{-1}(\mathbf{1}',\hat{\mathbf{1}}'') = -G_0^{-1}(\mathbf{1}',\hat{\mathbf{1}}'') + \gamma(\hat{\mathbf{1}}'',\mathbf{2},\hat{\mathbf{3}},\mathbf{4}) \times\Big[G_2(\mathbf{2},\hat{\mathbf{5}})G_2(\hat{\mathbf{3}},\mathbf{6}),G_2(\mathbf{4},\hat{\mathbf{7}})\Gamma_4(\hat{\mathbf{5}},\mathbf{6},\hat{\mathbf{7}},\mathbf{1}') + \sum_{\mathbf{i}=\hat{\mathbf{5}},\mathbf{6},\hat{\mathbf{7}}} G_2(\mathbf{2},\hat{\mathbf{5}})G_2(\hat{\mathbf{3}},\mathbf{6})G_2(\mathbf{4},\hat{\mathbf{7}})G_2(\tilde{\mathbf{9}},\widetilde{\mathbf{10}}) \times\Gamma_3(\tilde{\mathbf{9}},\mathbf{j}(\neq\mathbf{i}),\mathbf{k}(\neq\mathbf{i},\mathbf{j}))\Gamma_3(\widetilde{\mathbf{10}},\mathbf{1}',\mathbf{i}) + \sum_{\mathbf{i}=\mathbf{2},\hat{\mathbf{3}},\mathbf{4}} G_1(\mathbf{i})G_2(\mathbf{j}(\neq\mathbf{i}),\tilde{\mathbf{5}})G_2(\mathbf{k}(\neq\mathbf{i},\mathbf{j}),\widetilde{\mathbf{6}}) \times\Gamma_3(\tilde{\mathbf{5}},\tilde{\mathbf{6}},\mathbf{1}')\Big] + \gamma(\hat{\mathbf{1}}'',\mathbf{1}',\hat{\mathbf{3}},\mathbf{4})[G_2(\hat{\mathbf{3}},\mathbf{4}) + G_1(\hat{\mathbf{3}})G_1(\mathbf{4})] + \gamma(\hat{\mathbf{1}}'',\mathbf{2},\hat{\mathbf{3}},\mathbf{1}')[G_2(\mathbf{2},\hat{\mathbf{3}}) + G_1(\mathbf{2})G_1(\hat{\mathbf{3}})], \tag{5.6}$$

$$\Gamma_3(\mathbf{1}',\hat{\mathbf{1}}'',\tilde{\mathbf{1}}''')=\frac{\delta\Gamma_2(\mathbf{1}',\hat{\mathbf{1}}'')}{\delta G_1(\tilde{\mathbf{1}}''')}, \tag{5.7}$$

$$\Gamma_4(\mathbf{1}',\hat{\mathbf{1}}'',\mathbf{1}''',\hat{\mathbf{1}}^{\mathbf{iv}})=\frac{\delta^2\Gamma_2(\mathbf{1}',\hat{\mathbf{1}}'')}{\delta G_1(\mathbf{1}'''),\delta G_1(\hat{\mathbf{1}}^{\mathbf{iv}})}, \tag{5.8}$$

with $G_0(\mathbf{1},\hat{\mathbf{2}})$ defined as

$$G_0(\mathbf{1},\hat{\mathbf{2}})=\theta(t_1-t_2)\,\delta(\mathbf{k_1}-\mathbf{k_2})\exp[-D_0|t_1-t_2||\mathbf{k_1}-\mathbf{k_2}|^2].$$

The MSR G_0 above differs from its analogue in the direct perturbation calculation in Sec. II, because it is a function on two different sets of coordinates. The MSR Green's function is a measure of the response of the system at the coordinate labeled **1** to the introduction of density at coordinate $\hat{\mathbf{2}}$ so the zeros of the system are still arbitrary. The step function, $\theta(t)$, enforces causality and the δ function enforces translations invariance. To recover the usual Green's function with the creation event centered at the origin in real space at time $t=0$, we set $t_2=0$ and integrate over $\mathbf{k_2}$. The variables of the form $\tilde{\mathbf{i}}$ must be integrated over both arguments $\hat{\mathbf{i}}$ and $\mathbf{i}$, but many of the terms that they represent are zero. The result is similar to Deker's result for a cubic field at the second order [65]. For the second-order expression, we evaluate Γ_4 to first order. Γ_4 has two terms to first order.

$$\Gamma_4(\mathbf{1}',\hat{\mathbf{1}}'',\mathbf{1}''',\hat{\mathbf{1}}^{\mathbf{iv}})=\gamma(\hat{\mathbf{1}}'',\mathbf{1}',\hat{\mathbf{1}}^{\mathbf{iv}},\mathbf{1}''')+\gamma(\hat{\mathbf{1}}'',\mathbf{1}''',\hat{\mathbf{1}}^{\mathbf{iv}},\mathbf{1}').$$

We substitute this expression for Γ_4 in Eq. (5.5) and G_2 becomes

$$\begin{aligned}G_2(\mathbf{1}',\hat{\mathbf{1}}'')=&G_0(\mathbf{1}',\hat{\mathbf{1}}'')+G_0(\mathbf{1}',\hat{\mathbf{1}})\,\gamma(\hat{\mathbf{1}},\mathbf{2},\hat{\mathbf{3}},\mathbf{4})G_2(\mathbf{2},\hat{\mathbf{3}})G_2(\mathbf{4},\hat{\mathbf{1}}'')+G_0(\mathbf{1}',\hat{\mathbf{1}})\,\gamma(\mathbf{1},\mathbf{2},\mathbf{3},\mathbf{4})G_2(\mathbf{2},\hat{\mathbf{5}})G_2(\hat{\mathbf{3}},\mathbf{6})\\&\times G_2(\mathbf{4},\hat{\mathbf{7}})G_2(\hat{\mathbf{1}}'',\mathbf{8})\,\gamma(\hat{\mathbf{5}},\mathbf{6},\hat{\mathbf{7}},\mathbf{8})+G_0(\mathbf{1}',\hat{\mathbf{1}})\,\gamma(\mathbf{1},\mathbf{2},\mathbf{3},\mathbf{4})G_2(\mathbf{2},\hat{\mathbf{5}})G_2(\hat{\mathbf{3}},\mathbf{6})G_2(\mathbf{4},\hat{\mathbf{7}})G_2(\hat{\mathbf{1}}'',\mathbf{8})\,\gamma(\hat{\mathbf{5}},\mathbf{8},\hat{\mathbf{7}},\mathbf{6}).\end{aligned} \tag{5.9}$$

The last term is zero because it violates causality and it would be zero in the replica action because of the $N\to 0$ limit. Integrating over $\mathbf{k_{1''}}$ and setting $t_{1''}=0$ results in the second-order expression, which is identical to Eq. (2.3).

$$\begin{aligned}G(\mathbf{k},t)=&G_0(\mathbf{k},t)-\frac{(\beta D_0)^2}{(2\pi)^d}\int d\mathbf{h}d\tau_1 d\tau_2\{\mathbf{k}\cdot(\mathbf{k}-\mathbf{h})\mathbf{h}\cdot(\mathbf{k}-\mathbf{h})\chi(|\mathbf{k}-\mathbf{h}|,|\tau_1-\tau_2|)G_0(\mathbf{k},t-\tau_1)G(\mathbf{h},\tau_1-\tau_2)G(\mathbf{k},\tau_2)\}\\&+\frac{(\beta D_0)^4}{(2\pi)^{2d}}\int d\mathbf{h_1}d\mathbf{h_2}d\tau_1 d\tau_2 d\tau_3 d\tau_4\{\mathbf{k}\cdot(\mathbf{k}-\mathbf{h_1})\mathbf{h_2}\cdot(\mathbf{k}-\mathbf{h_1})\mathbf{h_1}\cdot(\mathbf{k}-\mathbf{h_1})(\mathbf{k}-\mathbf{h_1})\cdot(\mathbf{k}-\mathbf{h_1}+\mathbf{h_2})\chi(|\mathbf{k}-\mathbf{h_1}|,|\tau_1-\tau_3|)\\&\times\chi(|\mathbf{h_1}-\mathbf{h_2}|,|\tau_2-\tau_4|)G_0(\mathbf{k},t-\tau_1)G(\mathbf{h_1},\tau_1-\tau_2)G(\mathbf{h_2},\tau_2-\tau_3)G(\mathbf{k}-\mathbf{h_1}+\mathbf{h_2},\tau_3-\tau_4)G(\mathbf{k},\tau_4)\}.\end{aligned} \tag{5.10}$$

The average of $G(\mathbf{k},t)$ over disorder is implied. The perturbation expansion of the second-order term has a simple graphical expression that follows the notation used by Deker. As can be seen from the Dyson series above Eqs. (5.5)–(5.8), the MSR perturbation method expresses the Green's function in terms of a self-energy term, which explains the equivalence between the directly renormalized perturbation and the MSR results.

2. Two particle propagator

The first-order perturbation result with MSR is obtained from a simpler procedure than the direct perturbation result, but we do not determine a self-consistent equation. A self-consistent equation can be calculated with some complexity, but the definition of a two-particle propagator $G^{(1,2)}$ is a natural result of the vertex functions. We start by setting $N=2$ in the replica generating function and defining the two one-particle propagators, $G^{(1)}$ and $G^{(2)}$, where the superscripts have a similar meaning as Sec. II B, but $G^{(2)}$ does not contain $\exp[i\mathbf{k}\cdot\mathbf{r}]$. We also define a two-particle connected Green's function as

$$G_4(\mathbf{1}',\hat{\mathbf{2}}',\mathbf{3}',\hat{\mathbf{4}}')=\frac{\delta^4 Z[\xi_i,\hat{\xi}_i]}{\delta\xi_1(\mathbf{1}')\delta\hat{\xi}_1(\mathbf{2}')\delta\xi_2(\mathbf{3}')\delta\hat{\xi}_2(\mathbf{4}')}. \tag{5.11}$$

Similar to the one-particle propagator, we must add the initial conditions by setting $t_{2'}=t_{4'}=0$, multiplying by $\exp[i\mathbf{k}_{\mathbf{4}'}\cdot\mathbf{r}]$ and integrating over $\mathbf{k}_{\mathbf{4}'}$ and $\mathbf{k}_{\mathbf{2}'}$. Finally, we remove the primes on the labels and change the label of $\mathbf{k_3}$ to $\mathbf{k}_2$ to recover the first correction to the two-particle propagator which is captured in the expansion of the self-consistent equation, Eq. (2.4),

$$
\begin{aligned}
&G^{(1,2)}(\mathbf{k_1},t_1=t,\mathbf{k_2},t_2=t)\\
&\quad=G_2^{(1)}(\mathbf{k_1},t)G_2^{(2)}(\mathbf{k_2},t)\exp[i\mathbf{k_2}\cdot\mathbf{r}]\\
&\quad-\frac{(\beta D_0)^2}{(2\pi)^d}\int d\mathbf{h}\int_0^t d\tau_1\int_0^t d\tau_2\{\mathbf{k_1}\cdot(\mathbf{k_1}-\mathbf{h})\mathbf{k_2}\cdot(\mathbf{k_1}-\mathbf{h})\\
&\quad\times\chi(|\mathbf{k_1}-\mathbf{h}|,|\tau_1-\tau_2|)G^{(1)}(\mathbf{k_1},t-\tau_1)G^{(2)}(\mathbf{k_2},t-\tau_2)\\
&\quad\times G^{(1)}(\mathbf{h},\tau_1)G^{(2)}(\mathbf{k_1}+\mathbf{k_2}-\mathbf{h},\tau_2)\\
&\quad\times\exp[i(\mathbf{k_1}+\mathbf{k_2}-\mathbf{h})\cdot\mathbf{r}]\}. \qquad (5.12)
\end{aligned}
$$

C. MSR with replica trick and Gaussian reference system

The MSR perturbation is an asymptotic expansion, which may not have good accuracy at large disorder strengths. To overcome the difficulties of asymptotic expansions, several references introduce a variational technique that attempts to minimize the errors. These variational methods are referred to in the literature as the Gaussian reference technique [2,10,72,73]. To first order these techniques resemble the Edwards variational method. In the Gaussian reference technique the full action is fit with a different action that only contains a quadradic term, but the term is not necessarily Gaussian. The technique avoids the Dyson equation and the vertex renormalization used in Sec. V B. With the time dependent generating function for $Z^N[0,0]$ derived in Eq. (5.2) the Gaussian reference technique follows the same procedure as several references except that it is necessary to integrate over the time or frequency variable as well as the spatial variables [2,9,10]. The results of this technique are a time dependent analog of the results in these references and reduce to these previous results in the static disorder limit. For first order we get the first two terms derived in Eq. (5.9)

$$
\begin{aligned}
G_2(\mathbf{1}',\hat{\mathbf{1}}'')&=G_0(\mathbf{1}',\hat{\mathbf{1}}'')\\
&\quad+G_0(\mathbf{1}',\hat{\mathbf{1}})\,\gamma(\hat{\mathbf{1}},\mathbf{2},\hat{\mathbf{3}},\mathbf{4})G_2(\mathbf{2},\hat{\mathbf{3}})G_2(\mathbf{4},\hat{\mathbf{1}}''),
\end{aligned}
\qquad (5.13)
$$

but the second-order expression is more complex

$$
\begin{aligned}
2G_0(\mathbf{1}',\hat{\mathbf{1}}'')&=3G_2(\mathbf{1}',\hat{\mathbf{1}}'')-G_2(\mathbf{1}',\hat{\mathbf{1}})G_0^{-1}(\hat{\mathbf{1}},\mathbf{2})G_2(\mathbf{2},\hat{\mathbf{1}}'')+4G_0(\mathbf{1}',\hat{\mathbf{1}})\,\gamma(\hat{\mathbf{1}},\mathbf{2},\hat{\mathbf{3}},\mathbf{4})G_2(\mathbf{2},\hat{\mathbf{3}})G_2(\mathbf{4},\hat{\mathbf{1}}'')\\
&\quad-2G_2(\mathbf{1}',\hat{\mathbf{1}})\,\gamma(\hat{\mathbf{1}},\mathbf{2},\hat{\mathbf{3}},\mathbf{4})G_2(\mathbf{2},\hat{\mathbf{3}})G_2(\mathbf{4},\hat{\mathbf{1}}'')-G_2(\mathbf{1}',\hat{\mathbf{1}})\,\gamma(\hat{\mathbf{1}},\mathbf{2},\hat{\mathbf{3}},\mathbf{4})G_2(\mathbf{2},\hat{\mathbf{5}})G_0^{-1}(\hat{\mathbf{5}},\mathbf{6})G_2(\mathbf{6},\hat{\mathbf{3}})G_2(\mathbf{4},\hat{\mathbf{1}}'')\\
&\quad-G_0(\mathbf{1}',\hat{\mathbf{1}})\,\gamma(\hat{\mathbf{1}},\mathbf{2},\hat{\mathbf{3}},\mathbf{4})G_2(\mathbf{2},\hat{\mathbf{3}})G_2(\mathbf{4},\hat{\mathbf{5}})\,\gamma(\hat{\mathbf{5}},\mathbf{6},\hat{\mathbf{7}},\mathbf{8})G_2(\mathbf{6},\hat{\mathbf{7}})G_2(\mathbf{8},\hat{\mathbf{1}}'')\\
&\quad-G_0(\mathbf{1}',\hat{\mathbf{1}})\,\gamma(\hat{\mathbf{1}},\mathbf{2},\hat{\mathbf{3}},\mathbf{4})G_2(\mathbf{2},\hat{\mathbf{5}})\,\gamma(\hat{\mathbf{5}},\mathbf{6},\hat{\mathbf{7}},\mathbf{8})G_2(\mathbf{6},\hat{\mathbf{7}})G_2(\mathbf{8},\hat{\mathbf{3}})G_2(\mathbf{4},\hat{\mathbf{1}}'')\\
&\quad-G_0(\mathbf{1}',\hat{\mathbf{1}})\,\gamma(\hat{\mathbf{1}},\mathbf{2},\hat{\mathbf{3}},\mathbf{4})G_2(\mathbf{2},\hat{\mathbf{5}})G_2(\hat{\mathbf{3}},\mathbf{6})G_2(\mathbf{4},\hat{\mathbf{7}})G_2(\hat{\mathbf{1}}'',\mathbf{8})\,\gamma(\hat{\mathbf{5}},\mathbf{6},\hat{\mathbf{7}},\mathbf{8}).
\end{aligned}
\qquad (5.14)
$$

Expanding terms that contain G_0^{-1} or no G_0 demonstrates that this expression is the second-order perturbative term, Eq. (5.9), with additional third- and higher-order terms. These additional terms may improve the fit but they generally make numerically solving the self-consistent equations difficult by adding complexity to the equations. Because of this difficulty, we do not solve the second-order reference system calculation in this article.

The equality at second order is not unexpected because there is only one second-order graph that is not contained in the graphical expansion of the first-order self-consistent equation. The Gaussian reference method has many terms that appear redundant. At second order the terms cancel but they do not necessarily cancel at higher order. As a result, this method over counts some graphs and subtracts graphs that should be added. The expansion is also much more complicated and does not allow systematic diagrammatic analysis. Determining additional graphs to include in the expansion is difficult so expanding beyond second-order requires one to start from the third-order variational expression and reevaluate the higher-order terms.

VI. RENORMALIZATION GROUP RESULT

To further demonstrate the consistency of our results with other MSR methods, we perform a simple first-order renormalization group calculation to determine the effective diffusion constant. The calculation parallels several other one-loop approaches [2,58]. More sophisticated renormalization group calculations on the action in Eq. (5.2) have been used to determine the diffusion constant in static random media problems in several references as well [12,13]. Our approach is not general, but it allows the incorporation of dynamic disorder and the spirit of these calculations can be implemented for other forms of disorder. This approach also recovers the general form suggested by Dean and by Deem in the static limit, $\lambda\to 0$ [2,11].

The calculation begins by Fourier transforming the time variable, $t\to\omega$ so that $\mathbf{1}=[\mathbf{k_1},\omega_1]$ and $G_0^{-1}=i\omega+D|\mathbf{k}|^2$ in our generating function. Since the calculation is to first order we can take the number of replicas to be one. We introduce an artificial cutoff frequency in the spatial transform variable $\mathbf{k}$, denoted k_c, and define a momentum shell composed of frequencies that we eventually integrate over ($k_c/b\leqslant|\mathbf{k}|$

$\leqslant k_c$) with $b>1$. To first order we can replace $\hat{\rho}(\mathbf{i})\rho(\mathbf{j})$ with $|\mathbf{k_i}|, |\mathbf{k_j}| > k_c/b$ with $\delta(\mathbf{i}-\mathbf{j})(i\omega_i + D|\mathbf{k_i}|^2)^{-1}$. With these substitutions the action in our functional is

$$-G_0^{-1}(\mathbf{1},\mathbf{2})\hat{\rho}(\mathbf{1})\rho(\mathbf{2}) + \gamma(\mathbf{1},\mathbf{1}',\mathbf{1}',\mathbf{2})G_0(\mathbf{1}',\mathbf{1}')\hat{\rho}(\mathbf{1})\rho(\mathbf{2}) + \frac{1}{2}\gamma(\mathbf{1},\mathbf{2},\mathbf{3},\mathbf{4})\hat{\rho}(\mathbf{1})\rho(\mathbf{2})\hat{\rho}(\mathbf{3})\rho(\mathbf{4}) + \text{const}, \tag{6.1}$$

where the $\mathbf{1}'$ is integrated for $k_c/b \leqslant |\mathbf{k}'| \leqslant k_c$, the other $\mathbf{k}$ variables are integrated for $|\mathbf{k}| < k_c/b$, and all frequencies are integrated from $-\infty$ to ∞. The constant term comes from integrating the terms with $|\mathbf{k}| > k_c/b$ for all ρ and $\hat{\rho}$. This term only changes the normalization and will be omitted in further calculations.

Up to this point the random potential correlation function, χ has been general. Now we introduce the three-dimensional χ in Eq. (1.3) and evaluate the integrals over ω' and $\mathbf{k}'$. Integrating over ω' is done in a straightforward manner, but the $\mathbf{k}'$ integral has some difficulty. Since the final form should resemble a free diffusion propagator, we will perform a Taylor expansion of the integral in terms of $\mathbf{k_2}$ up to second order and assume the other terms are small. The new action is

$$\begin{aligned}
&-\int d\mathbf{1}d\mathbf{2}\left\{\delta(\mathbf{1}-\mathbf{2})\left[i\omega_2 + \left(D - \frac{4}{3\sqrt{2\pi}}(2\alpha)^{3/2}\chi_0\frac{(\beta D)^2}{D+\lambda}\int dr\left\{\left[2-\alpha r^2 - \frac{\lambda}{D+\lambda}\right]r^2\,\exp[-\alpha r^2]\right\}\right)|\mathbf{k_2}|^2\right]\hat{\rho}(\mathbf{1})\rho(\mathbf{2})\right\} \\
&\quad + \frac{1}{2}\left(\frac{\beta D}{(2\pi)^2}\right)^2\int d\mathbf{1}d\mathbf{2}d\mathbf{3}d\mathbf{4}\delta(\mathbf{1}-\mathbf{2}+\mathbf{3}-\mathbf{4})\left\{\mathbf{k_1}\cdot(\mathbf{k_1}-\mathbf{k_2})\mathbf{k_3}\cdot(\mathbf{k_3}-\mathbf{k_4})2(2\pi)^{3/2}(2\alpha)^{3/2}\chi_0\lambda|\mathbf{k_1}-\mathbf{k_2}|^2\right. \\
&\quad \left.\times\frac{\exp[-\alpha|\mathbf{k_1}-\mathbf{k_2}|^2]}{\lambda^2|\mathbf{k_1}-\mathbf{k_2}|^4 + (\omega_1-\omega_2)^2}\hat{\rho}(\mathbf{1})\rho(\mathbf{2})\hat{\rho}(\mathbf{3})\rho(\mathbf{4})\right\}
\end{aligned} \tag{6.2}$$

with $k_c/b < r = |\mathbf{k}| < k_c$ and $|\mathbf{k}| < k_c/b$. To get this result, a term of the form $[i\omega + (D+\lambda)r^2]^{-1}$ is replaced with $[(D+\lambda)r^2]^{-1}$ since r is large and the major contribution from ω is for $\omega \approx 0$. Rescaling $\mathbf{k}$ by b, ω by b^2 and the field variables, ρ and $\hat{\rho}$, by $b^{-7/2}$ results in an action with the same form as our original and the proper limits of integration.

$$\begin{aligned}
&-\int d\mathbf{1}d\mathbf{2}\left\{\delta(\mathbf{1}-\mathbf{2})\left[i\omega_2 + \left(D - \frac{4}{3\sqrt{2\pi}}(2\alpha)^{3/2}\chi_0\frac{(\beta D)^2}{D+\lambda}\int dr\left\{\left[2-\alpha r^2 - \frac{\lambda}{D+\lambda}\right]r^2\,\exp[-\alpha r^2]\right\}\right)|\mathbf{k_2}|^2\right]\hat{\rho}(\mathbf{1})\rho(\mathbf{2})\right\} \\
&\quad + \frac{1}{2b^3}\left(\frac{\beta D}{(2\pi)^2}\right)^2\int d\mathbf{1}d\mathbf{2}d\mathbf{3}d\mathbf{4}\delta(\mathbf{1}-\mathbf{2}+\mathbf{3}-\mathbf{4})\left\{\mathbf{k_1}\cdot(\mathbf{k_1}-\mathbf{k_2})\mathbf{k_3}\cdot(\mathbf{k_3}-\mathbf{k_4})2(2\pi)^{3/2}(2\alpha)^{3/2}\chi_0\lambda\right. \\
&\quad \left.\times|\mathbf{k_1}-\mathbf{k_2}|^2\frac{\exp\left[-\alpha\dfrac{\mu}{b^2}|\mathbf{k_1}-\mathbf{k_2}|^2\right]}{\lambda^2|\mathbf{k_1}-\mathbf{k_2}|^4 + (\omega_1-\omega_2)^2}\hat{\rho}(\mathbf{1})\rho(\mathbf{2})\hat{\rho}(\mathbf{3})\rho(\mathbf{4})\right\}
\end{aligned} \tag{6.3}$$

μ is a new scale factor that modulates the $|\mathbf{k}|^2$ term in the exponential. Before the first iteration of the renormalization group, $\mu = 1$. From this equation we determine the relationship between the old parameters and the new parameters, denoted with a prime.

$$\mu' \to \frac{\mu}{b^2},$$

$$\chi_0' \to \frac{\chi_0}{b^3}\left(\frac{D}{D'}\right)^2,$$

$$D' \to D - \frac{4}{3\sqrt{2\pi}}(2\alpha)^{3/2}\chi_0\frac{(\beta D)^2}{D+\lambda}\int dr \times\left\{\left[2-\alpha\mu r^2 - \frac{\lambda}{D+\lambda}\right]r^2\exp[-\alpha\mu r^2]\right\}.$$

By rescaling χ_0 by $(D/D')^2$ we replace the D^2 in the quartic term with $(D')^2$. Choosing $b = \exp[\Delta\zeta]$ with $\Delta\zeta \sim 0$ allows us to write approximate equations for the changes in these variables. These approximations will become accurate in the $\lim_{\Delta\zeta\to 0}$.

$$\Delta\mu \to -\mu 2\Delta\zeta,$$

$$\Delta\chi_0 \rightarrow -\chi_0 3\Delta\zeta + \chi_0^2 \frac{8}{3\sqrt{2\pi}}(2\alpha)^{3/2}\frac{(\beta D)^2}{D+\lambda} \times\left\{\left[2-\alpha\mu k_c^2-\frac{\lambda}{D+\lambda}\right]k_c^3\exp[-\alpha\mu k_c^2]\right\}\Delta\zeta,$$

$$\Delta D \rightarrow -\frac{4}{3\sqrt{2\pi}}(2\alpha)^{3/2}\chi_0\frac{(\beta D)^2}{D+\lambda} \times\left\{\left[2-\alpha\mu k_c^2-\frac{\lambda}{D+\lambda}\right]k_c^3\exp[-\alpha\mu k_c^2]\right\}\Delta\zeta.$$

The second term in the flow expression for χ_0 can be made arbitrarily small by choosing a large enough cutoff frequency k_c. This assumption fails when the μ becomes extremely small, but χ_0 can be arbitrarily small at the point of the failure, which allows us to neglect this term. This argument depends on the decay of χ_0 being faster than the decay of μ. From the first two equations, μ and χ_0 have a simple exponential form in terms of $\zeta = N\Delta\zeta$, where N is the number of iterations of the RG calculation.

$$\mu = \exp[-2\zeta],$$
$$\chi_0 = [\chi_0]_{\zeta=0}\exp[-3\zeta].$$

Substituting these expressions into the expression for D leads to the expression

$$\frac{dD}{d\zeta} = -\frac{4}{3\sqrt{2\pi}}(2\alpha)^{3/2}[\chi_0]_{\zeta=0}\frac{(\beta D)^2}{D+\lambda}\left\{\left[2-\alpha\ \exp[-2\zeta]k_c^2 - \frac{\lambda}{D+\lambda}\right]k_c^3\ \exp[-3\zeta]\ \exp[-\alpha\exp[-2\zeta]k_c^2]\right\}. \quad (6.4)$$

The new diffusion constant is the value of the solution to this equation at $\zeta=\infty$ with $D=D_0$ (the free diffusion value) at $\zeta=0$. The equation simplifies further by introducing a new variable of integration $k=-\sqrt{\alpha}k_c\ \exp[-\zeta]$, and defining dimensionless quantities $D'=D/D_0$ and $\lambda'=\lambda/D_0$. In the limit as the cutoff frequency goes to infinity, the initial conditions are $D'=1$ at $k=-\infty$, and the solution is D' at $k=0$. With these substitutions the equation for D' is straightforward in form.

$$\frac{dD'}{dk} = -\sigma\frac{k^2 D'^2}{D'+\lambda'}\left(2-k^2-\frac{\lambda'}{D'+\lambda'}\right)\exp[-k^2] \quad (6.5)$$

with

$$\sigma = \frac{8}{3\sqrt{\pi}}(\beta^2[\chi_0]_{\zeta=0}).$$

For $D\approx D_0$, the equation is just an integral and the result is the first-order nonrenormalized perturbation result

$$D = D_0 - D_0^2\frac{(D_0-\lambda)}{(D_0+\lambda)^2}\frac{\beta^2\chi_0}{3}. \quad (6.6)$$

This expression can also be derived by substituting $D=D_0$ in Eq. (3.3) and shows that the expression has the correct initial slope. The expression also recovers the static disorder limit ($\lambda\rightarrow 0$) reported in several references [2,10,11,49,50,58],

$$D = D_0\ \exp\left[-\frac{\beta^2\chi_0}{3}\right]. \quad (6.7)$$

A discussion of the comparison between the RG results and the perturbation results was presented in Sec. IV and are plotted in several figures, 1(b), 2(a), 2(b), 3(a), 3(b), and 3(c). As discussed in Sec. IV A, the RG calculation presented here gives the correct first-order perturbation result and examination of the flow equation, Eq. (6.5), demonstrates that the solution does not go to zero for finite disorder strength. As a result, the particle avoids trapping. As mentioned in Sec. IV A, the particle should exhibit this nontrapping behavior. The solution to this equation for the dynamic potential remains above $\exp[-\beta^2\chi_0/3]$, the static disorder solution in Eq. (6.7), which is also above the lower bound predicted by Masi *et al.* [2,57].

VII. DISCUSSION OF RESULTS

In this paper, we have extended previous MSR results for diffusion to a random potential with both spatial and temporal correlations. We perform a Dyson expansion to develop renormalized propagators for one- and two-particle systems. These propagators determine the characteristics of the system including the diffusion constant and non-Gaussian indicators. Most of the results are general for arbitrary dynamic potential correlation function χ or can be generalized by following the spirit of these calculations.

The field theoretic method developed by Martin, Siggia, and Rose is shown to be consistent with the direct Dyson expansion. A perturbation expansion using the MSR method yields the same single-particle propagator to second order and the same first-order expression for the two-particle propagator. The field theoretic method of MSR can also be used to determine an Edwards type of variational fit of the propagator, which has the same first-order expression as perturbation but a more complicated second-order expression. The variational approach is also consistent with previous static calculations [2]. The diffusion constant is also determined from a renormalization group calculation. These results are consistent with previous work in the static limit and give a reasonable generalization to dynamic disorder [2,11].

The renormalized perturbation expansion used to determine the diffusion constant demonstrates the expected behavior of a perturbation expansion. The results match the nonrenormalized expansion for small values of disorder strength but eventually they deviate from reasonable behavior and predict trapping. The dynamics of the potential correlation functions, λ, increased the diffusion constant because any barriers to diffusion would eventually rearrange, allowing the particle to move, but the renormalized perturbation expansion still predicts trapping for finite disorder strength. A renormalization group calculation with the MSR formalism shows more reasonable behavior with the diffu-

sion constant decreasing as an exponential with respect to the disorder strength in the static limit, which is consistent with previous calculations and simulations, and as a power law for a system with nonzero λ [2].

The correlations functions determined by the perturbation expansions for the two-particle Green's functions exhibit collective behaviors that can be interpreted as clustering in this model. Particles that originate near each other have a tendency to diffuse with similar rates and move closer together. This behavior results in long lived correlations that are apparent even in the nonrenormalized expressions. Since perturbation expansions have a tendency to over emphasize the effects of the potential, we expect that the renormalized propagator will demonstrate even stronger correlations between the particles.

Although the model was chosen for computational convenience, the correlations exhibit behaviors that are similar to real systems like glasses and supercritical fluids. This study also demonstates that the anayltical and computational methods used in this paper can be applied to the diffusion of a solute in real systems with a potential-potential correlation function determined for these systems.

ACKNOWLEDGMENTS

This research is supported by the AT&T Research Fund Award and the NSF Career Award (Grant No. Che-0093210). We thank P. Geissler for useful discussions.

[1] J.P. Bouchaud *et al.*, J. Phys. (Paris) **48**, 1445 (1987).
[2] M.W. Deem and D. Chandler, J. Stat. Phys. **76**, 911 (1994).
[3] I.T. Drummond *et al.*, J. Fluid Mech. **128**, 75 (1984).
[4] D.L. Koch and E.S.G. Shaqfeh, Phys. Fluids A **4**, 887 (1992).
[5] K.G. Wang, J. Phys. A **27**, 3655 (1994).
[6] R.H. Kraichnan, Phys. Fluids **13**, 22 (1970).
[7] R. Phythian, J. Fluid Mech. **67**, 145 (1975).
[8] R. Phythian, J. Fluid Mech. **89**, 241 (1978).
[9] J.P. Bouchaud and A. Georges, Phys. Rep. **195**, 127 (1990).
[10] M.W. Deem, Phys. Rev. E **51**, 4319 (1995).
[11] D.S. Dean *et al.*, J. Phys. A **27**, 5135 (1994).
[12] V.E. Kravtsov *et al.*, J. Phys. A **18**, L703 (1985).
[13] V.E. Kravtsov *et al.*, Phys. Lett. A **119**, 203 (1986).
[14] R.M. Dickson *et al.*, Science **274**, 966 (1996).
[15] X. Xu and E.S. Yeung, Science **275**, 1106 (1997).
[16] E.R. Weeks *et al.*, Science **287**, 627 (2000).
[17] B. Cui *et al.*, J. Chem. Phys. **114**, 9142 (2001).
[18] A.H. Marcus *et al.*, Phys. Rev. E **60**, 5725 (1999).
[19] G. Hinze and H. Sillescu, J. Chem. Phys. **104**, 314 (1996).
[20] A.M. Boiron *et al.*, Chem. Phys. **247**, 119 (1999).
[21] E. Barkai *et al.*, Phys. Rev. Lett. **84**, 5339 (2000).
[22] R. van Zon and J. Schofield, Phys. Rev. E **65**, 011106 (2002).
[23] M.D. Ediger, Annu. Rev. Phys. Chem. **51**, 99 (2000).
[24] B. Doliwa and A. Heuer, Phys. Rev. Lett. **88**, 4915 (1998).
[25] C. Donati *et al.*, Phys. Rev. Lett. **82**, 627 (1999).
[26] C. Donati *et al.*, Phys. Rev. E **60**, 3107 (1999).
[27] T.R. Kirkpatrick *et al.*, Phys. Rev. A **40**, 1045 (1989).
[28] A. Kasper *et al.*, Langmuir **14**, 5004 (1998).
[29] R. van Zon and J. Schofield, Phys. Rev. E **65**, 011107 (2002).
[30] A. Tolle and H. Sillescu, Langmuir **10**, 4420 (1994).
[31] J. Kanetakis *et al.*, Phys. Rev. E **55**, 3006 (1997).
[32] R.S. Urdahl *et al.*, J. Chem. Phys. **105**, 8973 (1996).
[33] D.D. Brace *et al.*, J. Chem. Phys. **116**, 1598 (2002).
[34] S.C. Tucker, Chem. Rev. **99**, 391 (1999).
[35] A. Cunsolo *et al.*, J. Chem. Phys. **114**, 2259 (2001).
[36] A.A. Clifford and S.E. Coleby, Proc. R. Soc. London, Ser. A **433**, 63 (1991).
[37] S. De *et al.*, Chem. Eng. Sci. **56**, 5003 (2001).
[38] G. Goodyear and S.C. Tucker, J. Chem. Phys. **111**, 9673 (1999).
[39] A.N. Drozdov and S.C. Tucker, J. Chem. Phys. **114**, 4912 (2001).
[40] C.Z. Liu and I. Oppenheim, Proc. Natl. Acad. Sci. U.S.A. **94**, 7927 (1997).
[41] R. Zwanzig, Chem. Phys. Lett. **164**, 639 (1989).
[42] J. Cao, Phys. Rev. E **63**, 041101 (2001).
[43] E. Zaccarelli *et al.*, Europhys. Lett. **55**, 157 (2001).
[44] S.C. Glotzer *et al.*, J. Chem. Phys. **112**, 509 (2000).
[45] J. Wu and J. Cao, Phys. Rev. E (to be published).
[46] G. Tarjus and D. Kielson, J. Chem. Phys. **103**, 3071 (1995).
[47] J.D. Gezelter *et al.*, J. Chem. Phys. **110**, 3444 (1999).
[48] E. Rabani *et al.*, J. Chem. Phys. **107**, 6967 (1997).
[49] D.S. Dean *et al.*, J. Phys. A **28**, 6013 (1995).
[50] V. Pham and M.W. Deem, J. Phys. A **31**, 7235 (1998).
[51] P.H. Roberts, J. Fluid Mech. **11**, 257 (1961).
[52] D.L. Kock and J.F. Brady, Phys. Fluids A **1**, 47 (1989).
[53] R.P. Feynman, Phys. Rev. **76**, 769 (1949).
[54] M. Tokuyama *et al.*, Physica A **270**, 380 (1999).
[55] J.C. Crocker *et al.*, Phys. Rev. Lett. **85**, 888 (2000).
[56] M.J. Solomon and Q. Lu, Curr. Opin. Colloid Interface Sci. **6**, 430 (2001).
[57] A.D. Masi *et al.*, J. Stat. Phys. **55**, 787 (1989).
[58] L. Chen *et al.*, J. Phys. Chem. B **104**, 6033 (2000).
[59] P.C. Martin *et al.*, Phys. Rev. A **8**, 423 (1973).
[60] R. Phythian, J. Phys. A **8**, 1423 (1975).
[61] R.V. Jensen, J. Stat. Phys. **25**, 183 (1981).
[62] C.D. Dominicis and L. Peliti, Phys. Rev. B **18**, 353 (1978).
[63] C.D. Dominicis, Phys. Rev. B **18**, 4913 (1978).
[64] C.A.K. *et al.*, J. Chem. Phys. **100**, 1528 (1994).
[65] U. Deker, Phys. Rev. A **19**, 846 (1979).
[66] U. Deker and F. Haake, Phys. Rev. A **11**, 2043 (1975).
[67] U. Deker and F. Haake, Phys. Rev. A **12**, 1629 (1975).
[68] R. Phythian, J. Phys. A **9**, 239 (1976).
[69] R. Phythian, J. Phys. A **10**, 777 (1977).
[70] H.-K. Janssen, Z. Phys. B **23**, 377 (1976).
[71] H.C. Andersen, J. Math. Phys. **41**, 1979 (2000).
[72] O. Parcollet *et al.*, Phys. Rev. B **53**, 3161 (1996).
[73] M. Barthelemy and H. Orland, Physica A **207**, 106 (1994).